

Supporting Information

Solution-Processable Porous Graphitic Carbon from Bottom-Up Synthesis and Low-Temperature Graphitization

Sai Che,^{a,c} Chenxuan Li,^a Chenxu Wang,^b Wasif Zaheer,^a Xiaozhou Ji,^a Bailey Phillips,^a Guvanch Gurbandurdyev,^a Jessica Glynn,^a Zi-Hao Guo,^d Mohammed Al-Hashimi,^e Hong-Cai Zhou,^{a,b} Sarbajit Banerjee,^{*a,b} and Lei Fang^{*a,b}

^aDepartment of Chemistry, ^bDepartment of Materials Science & Engineering, Texas A&M University, College Station, Texas 77843, USA

^cState Key Laboratory of Heavy Oil Processing, China University of Petroleum, Beijing 102249, China

^dSouth China Advanced Institute for Soft Matter Science and Technology, South China University of Technology, Guangzhou 510640, China

^eDepartment of Chemistry, Texas A&M University at Qatar, P. O. Box 23874, Doha, Qatar

Email: banerjee@chem.tamu.edu; fang@chem.tamu.edu

Table of Contents

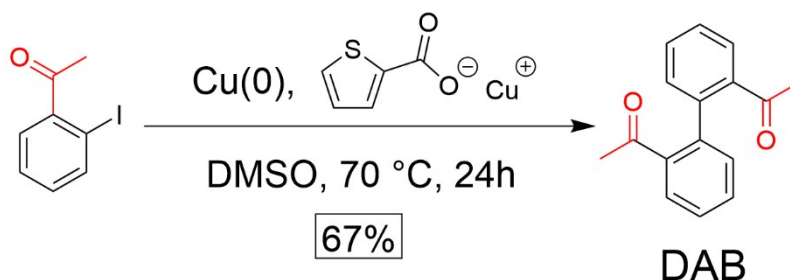
1. General Information.....	S3
2. Synthesis.....	S4
3. Porosity Measurements and Stability Tests.....	S6
4. Fourier Transform Infrared Spectroscopy (FT-IR).....	S8
5. Solid-State NMR.....	S9
6. X-ray absorption near-edge structure (XANES).....	S10
7. Scanning Electron Microscope (SEM) Images.....	S11
8. Conductivity.....	S13
9. X-ray Photoelectron Spectroscopy (XPS).....	S16
10. Elemental Analysis.....	S19
11. Reference.....	S20

1. General Information

Starting materials, reagents, and solvents were purchased from Aldrich, Alfa Aesar, TCI, and Acros, and were used as received without further purification unless otherwise specified. Analytical thin-layer chromatography (TLC) tests were performed on glass that was precoated with silica gel 60-F254 (Sorbtech). Flash column chromatography was carried out using a Biotage® Isolera™ Prime. Solution phase ¹H- and ¹³C-NMR spectra were obtained on Bruker Ascend 400 MHz spectrometers at room temperature. Chemical shifts are reported in ppm relative to the signals corresponding to the residual non-deuterated solvents (for ¹H NMR: CDCl₃ δ = 7.26 ppm; for ¹³C NMR: CDCl₃ δ = 77.16 ppm). High-resolution Atmospheric Pressure Chemical Ionization (HR-APCI) mass spectra were performed using a Thermo Fisher Scientific Q Exactive Focus. Thermogravimetric analysis (TGA) data were collected on Mettler-Toledo TGA-DSC-1 at a heating rate of 20 °C min⁻¹ from 30 °C to 900 °C under N₂ atmosphere. Powder X-ray diffraction (PXRD) was obtained with a Bruker D8-Focus Bragg-Brentano X-ray Powder Diffractometer equipped with a Cu sealed tube (λ = 1.54178 Å) at 40 kV and 40 mA.

2. Synthesis

Monomers Synthesis



DAB: A mixture of 1-(2-iodophenyl)ethan-1-one (12.3 g, 50 mmol), Cu powder (31.8 g, 500 mol) and Copper(I) thiophene-2-carboxylate (47.7 g, 250 mmol) in DMSO (500 mL) was heated at 70 °C for 24 h. After the reaction was cooled down to room temperature, the precipitate was filtered out. The filtrate was poured into water. The white precipitate was filtered and washed with water. The crude product was purified by column chromatography (SiO₂, hexanes : EtOAc = 5:1) to yield **DAB** as a white solid (4.0 g, 67%). ¹H NMR (400 MHz, Chloroform-*d*): δ 7.73 (dd, *J* = 7.5, 1.7 Hz, 2H), 7.52-7.41 (m, 4H), 7.16 (dd, *J* = 7.5, 1.7 Hz, 2H), 2.25 (s, 2H). ¹³C NMR (100 MHz, Chloroform-*d*): δ 201.68, 140.68, 138.76, 131.11, 130.78, 128.62, 127.67. HRMS (APCI): calcd for C₁₆H₁₄O₂ [*M*+H]⁺ *m/z*=239.1067; found *m/z*=239.1063.

PGC-Pr: A 20 mL vial was charged with **DAB** (0.50 g, 2.1 mmol) and MSA (3 mL). The mixture was sonicated for 5 min. The resulting orange solution was heated to 90 °C for 1 h. Then the temperature was increased to 150 °C and kept for 24 h in a flask open to the air. The black solid was filtered, washed with methanol, and further washed by boiling THF in a Soxhlet extractor. The remaining solid was vacuum dried to give a black solid **PGC-Pr** (0.41 g, quantitative). Subsequently, the solid was annealed at various temperatures under N₂ for 3 h to afford **PGT-T** (**PGC-300**, **PGC-400**, **PGC-500**, **PGC-600**, **PGC-700**, **PGC-800**, and **PGC-1000** respectively). N₂ flow rate: 100 mL min⁻¹. Temperature ramp rate: 2 °C min⁻¹.

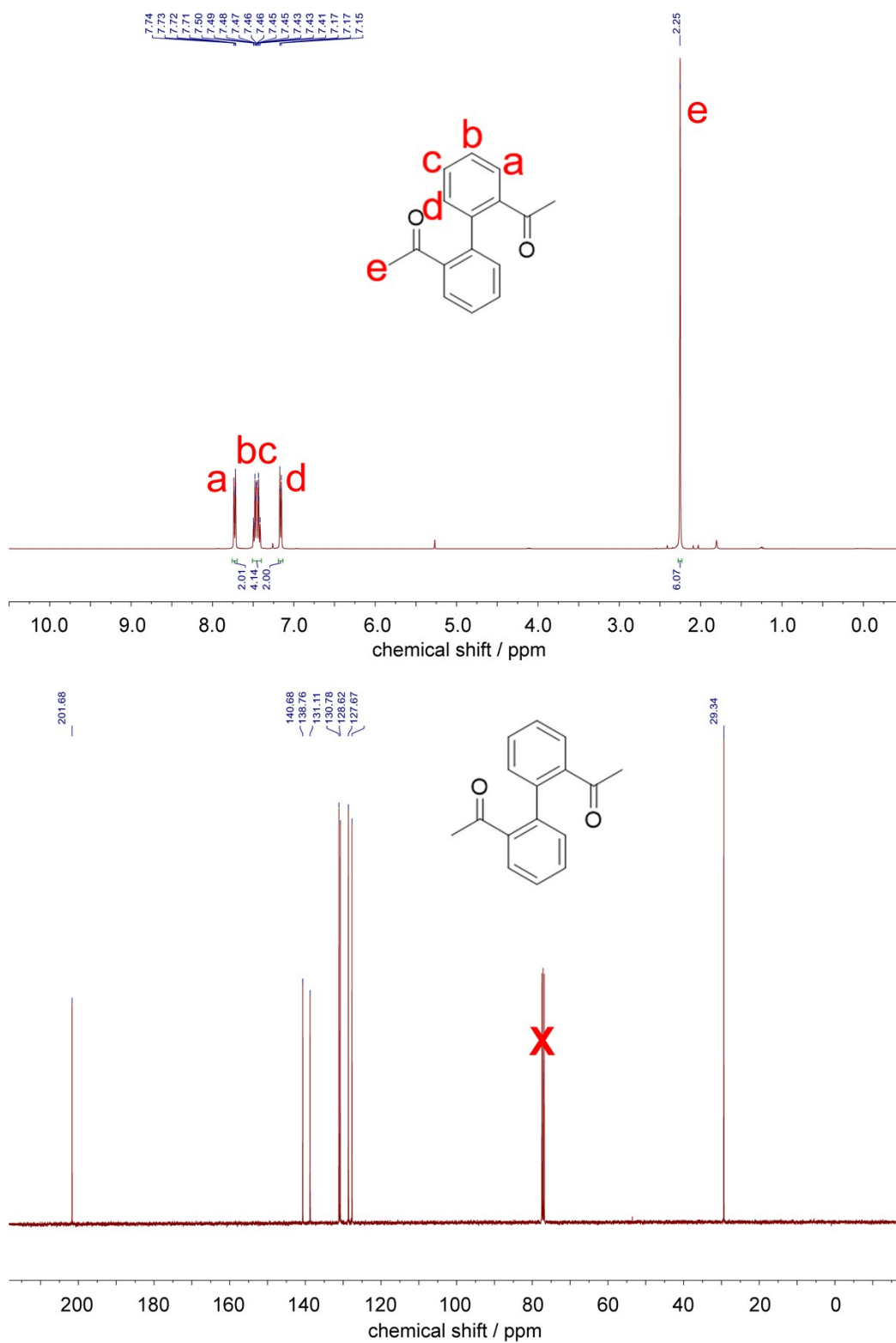


Figure S1. ^1H (400 MHz, CDCl_3 , RT) and ^{13}C NMR (100 MHz, CDCl_3 , RT) spectra of DAB monomer.

3. Porosity Measurements and Stability Tests

N_2 sorption isotherms at 77 K were measured with a Micromeritics ASAP 2020 surface area and pore size analyzer. Prior to the gas adsorption measurements, the sample was degassed for 10 h at 120 °C. All three materials showed type I isotherms in the lower pressure region with increased adsorption at higher pressure. The partial pressure range for the calculation of Brunauer-Emmett-Teller (BET) specific surface areas of samples was obtained from the corresponding Rouquerol plots, where the $V(1-P/P_0)$ is continuously increasing along with P/P_0 .¹⁻² Pore size distribution data were calculated from the N_2 sorption isotherms based on the Nonlocal Density Functional Theory (NLDFT) method in the Micromeritics ASAP 2020 software package (assuming slit pore geometry).¹ All three materials showed primarily micropores at 1.2 ~ 1.5 nm, with a small population of broadly distributed mesopores. Due to the amorphous nature and possible interpenetration, the pore sizes and their distributions were not heavily dependent on their ideal crystalline structures. The mesopores were attributed to reaction defects formed during the Suzuki polymerization and interparticulate voids of the amorphous solid.³

Standard procedure: **PGC-800** (50 mg) solid material was suspended in 10 mL of each following solutions (1) 12 M HCl at 80 °C for 7 days; (2) 14 M NaOH in $H_2O/MeOH$ at 80 °C for 7 days; (3) 50 equiv. $NaBH_4$ in MeOH at 80 °C for 7 days; (4) chromic acid solution (0.1 M $K_2Cr_2O_7$ in concentrated H_2SO_4) for 3 days; or (5) 98% TfOH for 7 days. Afterwards, the solid material was collected by filtration, washed with H_2O and MeOH, and dried in vacuum. Subsequently, the remaining solid was subjected to solid state CP-MAS NMR and nitrogen adsorption isotherm tests.

As expected for a graphitic carbon-based material, **PGC-800** demonstrated excellent stability after extended treatments in harsh chemical conditions, including acids (12 M HCl at 80 °C, 7 days; or 98% TfOH, 7 days), base (14 M NaOH in $H_2O/MeOH$ at 80 °C, 7 days), reducing agent (50 equiv. $NaBH_4$ in MeOH at 80 °C, 7 days), and oxidant (0.1 M $K_2Cr_2O_7$ in concentrated H_2SO_4). BET surface area and conductivity remained mostly intact through all treatments, demonstrating that the fully graphitized backbone endowed the material with exceptional chemical stability.

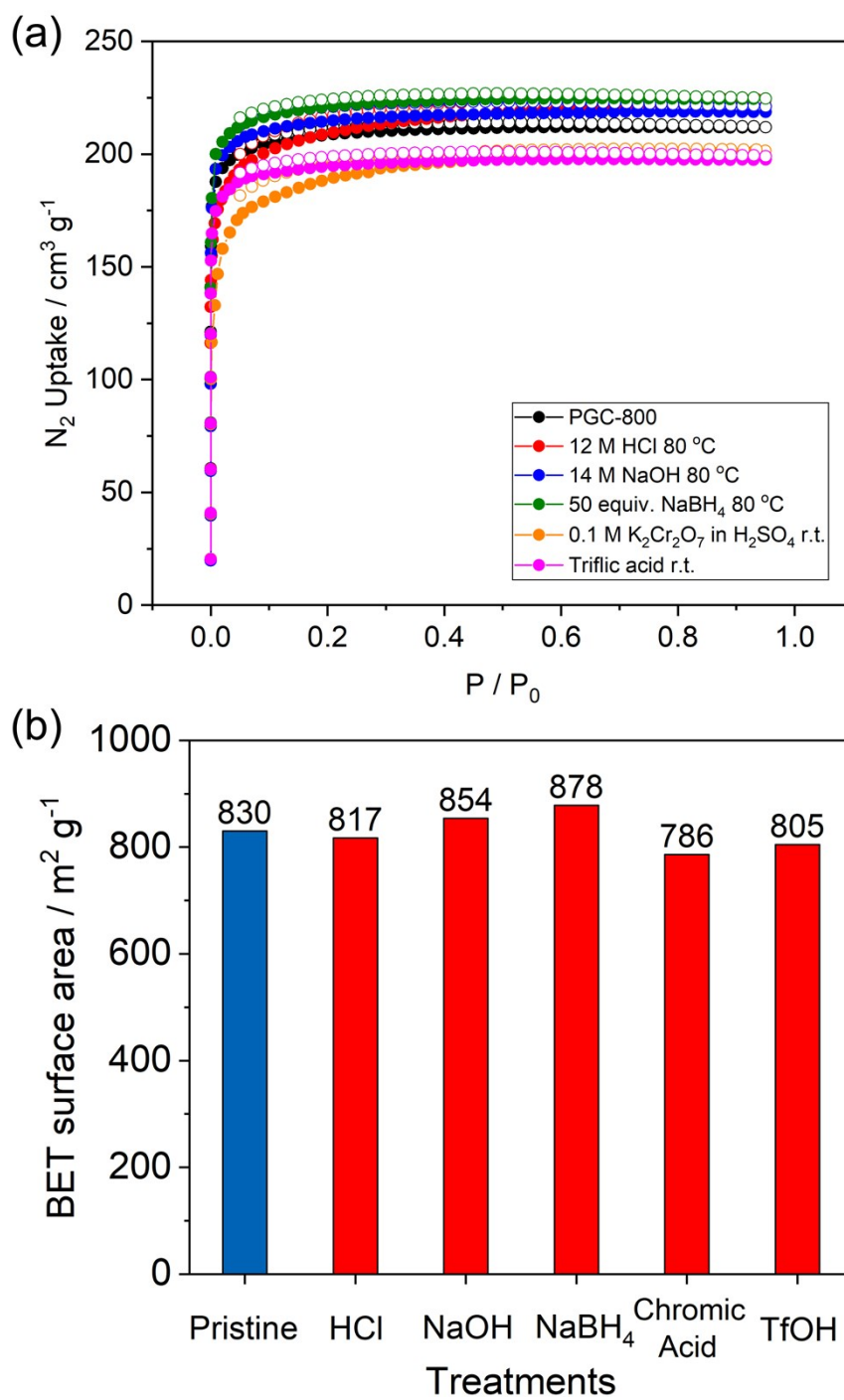


Figure S2. N₂ adsorption isotherms (a) and BET surface areas (b) of **PGC-800** after each treatment.

4. Fourier Transform Infrared Spectroscopy (FT-IR)

Fourier transform infrared spectroscopy (FT-IR) spectra were recorded by ZnSe attenuated total reflection on a Shimadzu IRAffinity-1S spectrometer. FT-IR peaks corresponding to aromatic carbonyl groups at 1670–1707 cm^{-1} were observed in both monomer **DAB** and **PGC-Pr**, indicating the incomplete conversion of the ATC reaction. The fingerprint feature of 1,2-disubstituted benzene rings at 748 cm^{-1} and 1,3,5-trisubstituted benzene rings at 880, 810, and 695 cm^{-1} were observed in **PGC-Pr**,⁴ due to the incomplete graphitization without annealing.

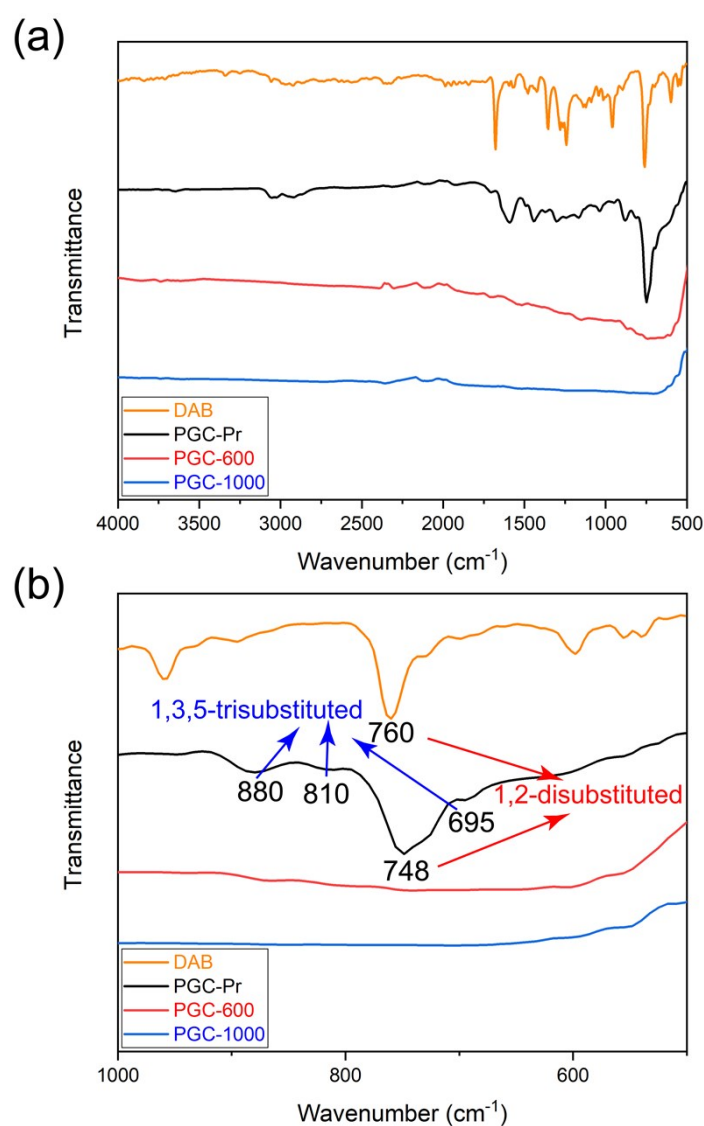


Figure S3. Full FT-IR spectra (a) and aromatic fingerprint region FTIR spectra of **DAB**, **PGC-Pr**, **PGC-600**, and **PGC-1000**.

5. Solid-State NMR

Solid-state CP/MAS ^{13}C NMR spectra were obtained on a Bruker Avance 400 MHz spectrometer with 4 mm CP/MAS probes and MAS rates of 10 kHz at room temperature. The spectra of **DAB** showed the signal of sp^3 methyl groups at 30 ppm and acetyl groups (C=O) at 200 ppm (the splitting was ascribed to the rotamers), while no distinct signals were observed for **PGC-Pr**, indicating the high degree of polymerization.⁵ Both **PGC-Pr** and **PGC-600** showed peaks in 120-130 ppm range, indicating the dominant presence of sp^2 carbons. The peak of **PGC-1000** was not measurable due to the presence of strong paramagnetism.

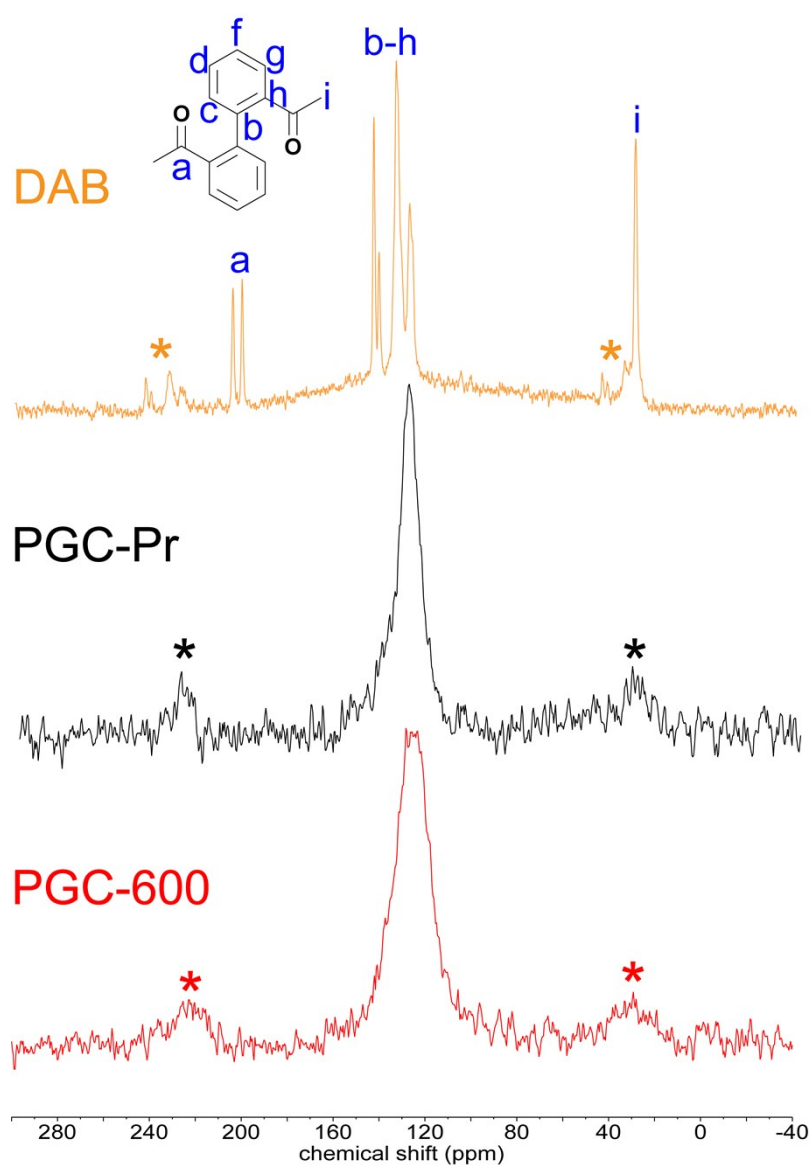


Figure S4. Solid-state CP/MAS ^{13}C NMR spectra of **DAB**, **PGC-Pr** and **PGC-600**.

6. X-ray absorption near-edge structure (XANES)

C K- and O K- XANES measurements were carried out at the National Synchrotron Light Source II of Brookhaven National Laboratory beamline SST-1 operated by the National Institute of Standards and Technology. Measurements were performed in partial electron yield (PEY) mode with a nominal resolution of 0.1 eV. The PEY signal was normalized to the incident beam intensity of a clean gold grid to eliminate the effects of any incident beam fluctuations and optics absorption features. The π^* feature in the O K-edge data represents the transition of O 1s electrons to π^* C=O states derived from the acetyl groups. The decrease in the intensity of this feature for **PGC-600** relative to **PGC-Pr** points to a loss of C=O moieties. The broad feature centered at 540.7 eV can be assigned to the transitions of O 1s core-level electrons to σ^* C–O and C=O states of acetyl groups and other oxygen-containing functionalities.

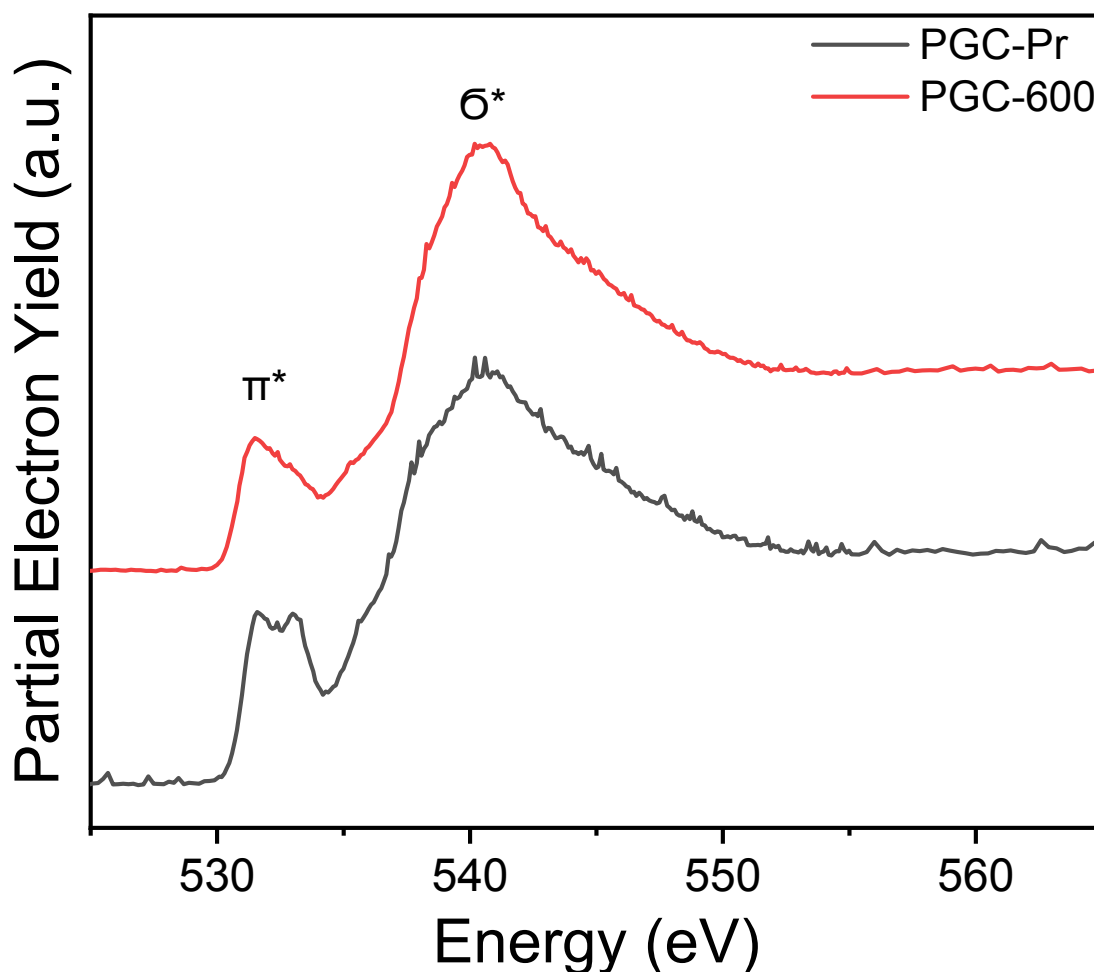


Figure S5. XANES data at the O K-edge of PGC-Pr and PGC-600.

7. Film Fabrication and Scanning Electron Microscope (SEM) Images

DAB monomer (150 mg) was dissolved in MSA (1 mL) to form the reaction solution. The solution was drop-cast onto a 6" X 6" glass substrate and sandwiched between another piece of glass of the same size. These glass substrates were pre-treated by spraycoating a thin layer of PTFE to prevent undesired adhesion of the membrane onto the glass. Two pieces of 150 mm-thick micro cover glass slides were placed in between (Figure S5a). The sandwiched system was heated at 110 °C for 24 h. After the reaction, the freestanding **PGC** membrane was detached from the glass substrate and soaked in methanol for 45 min. It was then taken out and soaked in another batch of clean methanol. After repeating twice, the membrane was dried in air. The following annealing processes were conducted under the same condition as power samples. Field-emission scanning electron microscopic (SEM) images were collected using the FEI Quanta 600 FE-SEM.

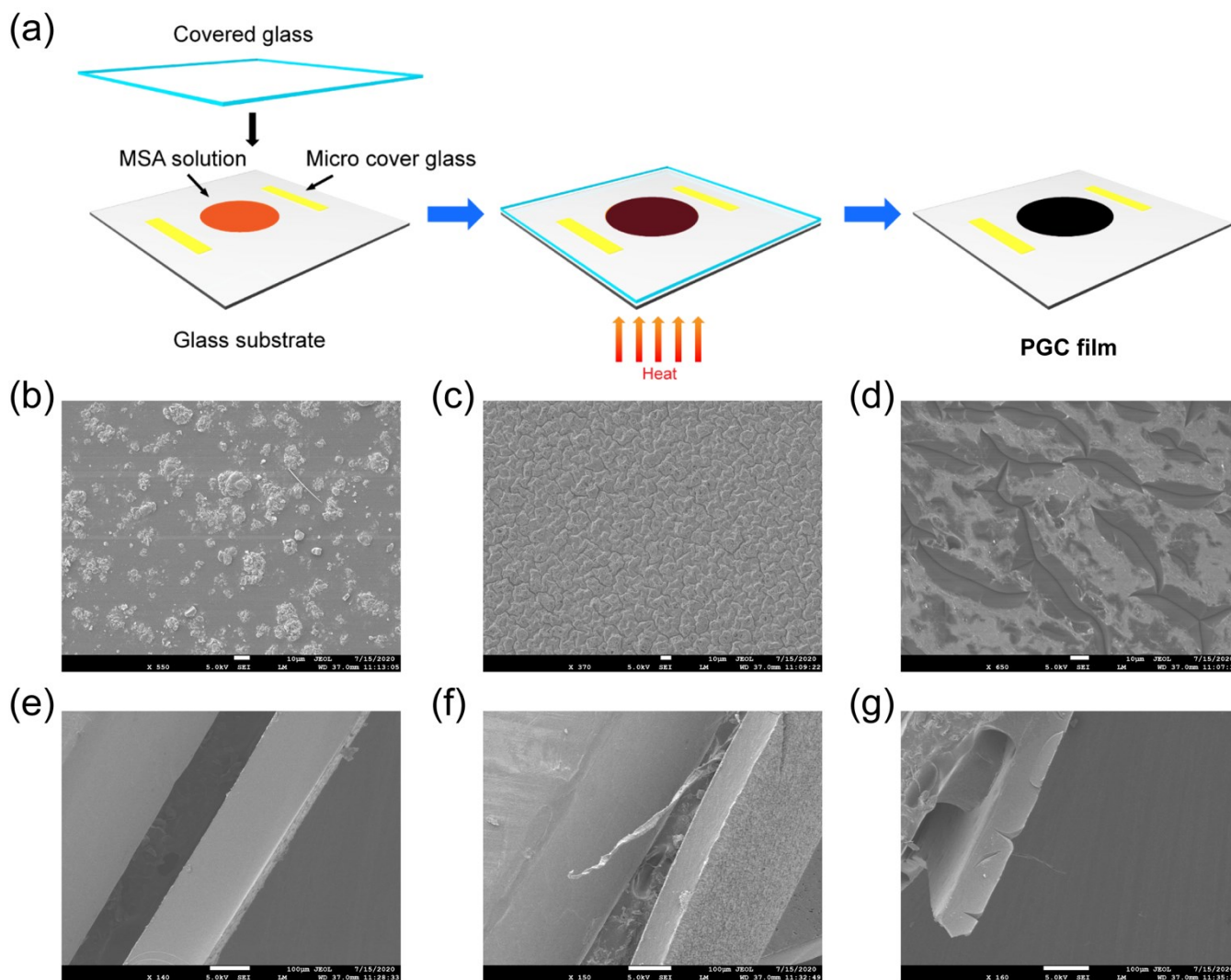
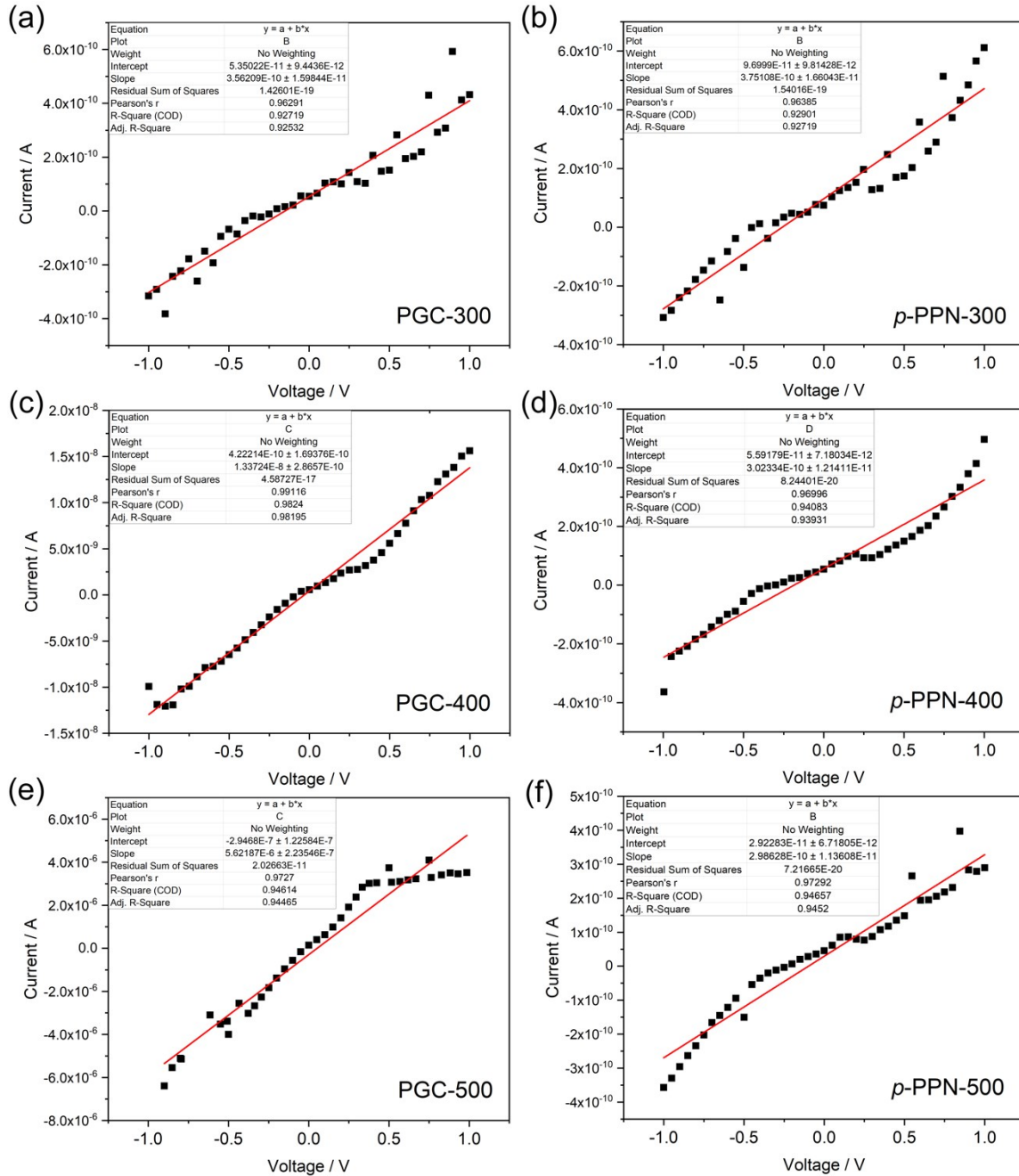


Figure S6. (a) Graphic representation of thin film fabrication using an MSA solution of the monomer. Top view SEM images of **PGC** film (b), **PGC-600** film (c), and **PGC-1000** film (d). Cross-sectional view SEM images of **PGC** film (e), **PGC-600** film (f), and **PGC-1000** film (g).

8. Conductivity

Conductivity of PGC and *p*-PPN films was evaluated by a four-point probe method. The electrical resistance was measured with a Keithley 2450 SourceMeter. The thickness of the pellet was measured using scanning electron microscopy. The electrical conductivity was calculated based on the slope of the I-V plots.



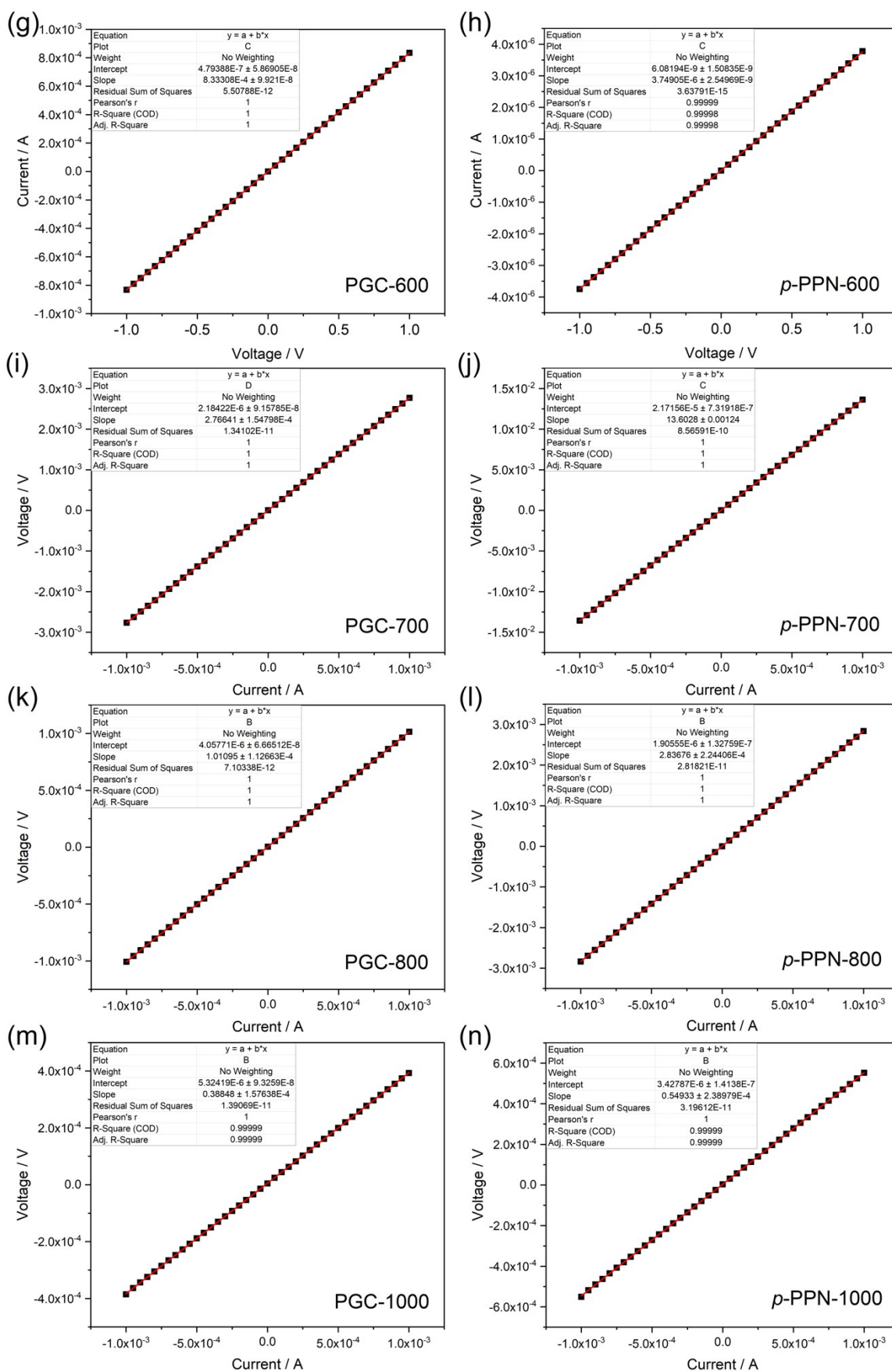


Figure S7. I-V plots from 4-probe conductivity measurement of PGC and p-PPN films pyrolyzed at different temperatures.

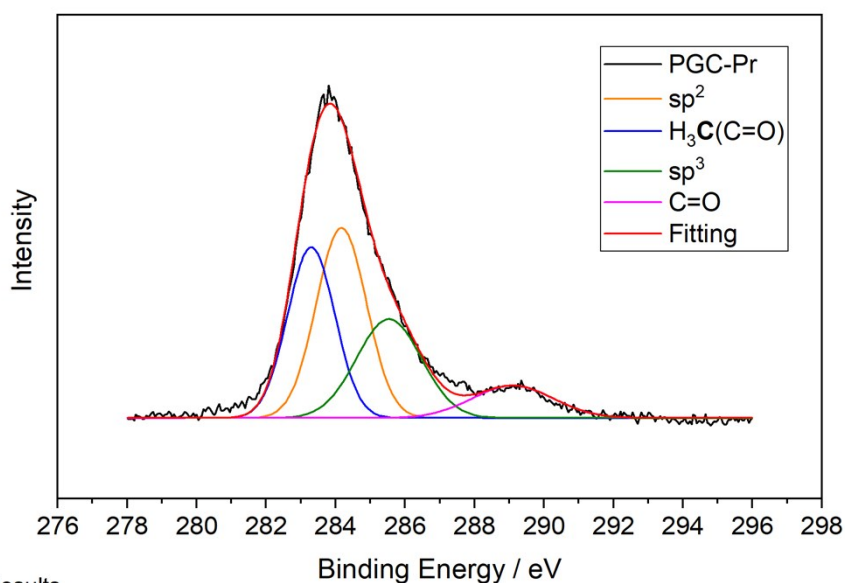
Table S1. Electrical conductivity comparison of reported porous carbons.

Name	Pyrolysis Temperature / °C	Electrical Conductivity / S cm ⁻¹	Reference
PGC-300	300	1.31 X 10 ⁻⁸	This work
PGC-400	400	4.92 X 10 ⁻⁷	
PGC-500	500	2.07 X 10 ⁻⁴	
PGC-600	600	0.031	
PGC-700	700	13.3	
PGC-800	800	36.4	
PGC-1000	1000	94.8	
RuO ₂ /ACNF	800	0.59	6
PPS α -CD	800	0.62	7
URC-700	700	~0	8
URC-800	800	~0.25	
URC-900	900	~2.75	
URC-1000	1000	~4.10	
URC-1100	1100	~4.40	
1300-CC 1300-Ni-GCM 1300-Ani-GCM	1300	14.97 25.75 24.75	9
NGPCs-850	850	6.93	10
PAC-10	1000	6.23	11
GPAN-1000 GPAN-1800 GPAN-2200	1000 1800 2200	5.32 51.01 75.91	12
C-800	900	0.19	13
C-1400-3	1400	54.5	14

9. X-ray Photoelectron Spectroscopy (XPS)

X-ray photoelectron spectroscopy (XPS) analysis was carried out with Omicron XPS/UPS system with Argus detector using Omicron's DAR 400 dual Mg/Al X-ray source. The deconvoluted C 1s spectra were assigned as follows: 283.3 eV for carbon of the acetyl groups [$\text{H}_3\text{C}(\text{C}=\text{O})$], 284.4 eV for sp^2 carbon, 285.4 eV for sp^3 carbon, 289.1 eV for C=O, 287.7 eV for O-C-O.¹⁵⁻¹⁶ **DAB** monomer showed the corresponding ratio of 2:2:12 for methyl:acetyl (C=O):biphenyl groups. Without pyrolysis, **PGC-Pr** was revealed to have decent amount of acetyl groups. Pyrolysis significantly diminished acetyl groups, and the ratio of sp^2/sp^3 carbon increased from 1.485 (**PGC-Pr**) to 1.847 (**PGC-600**) to 3.745 (**PGC-1000**), confirming the increased degree of graphitization.

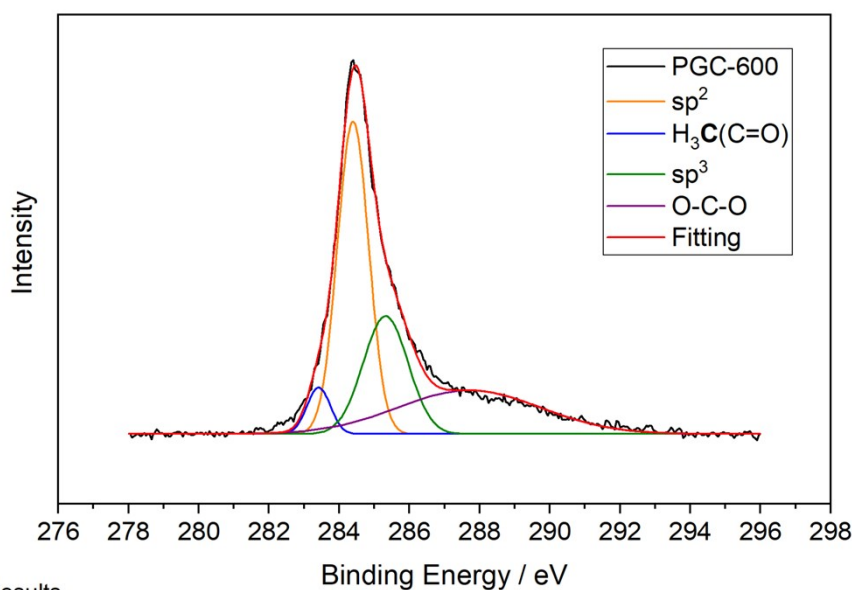
(a) BaseLine:Tougaard
 Chi²=3.19811E+004 Adj. R-Square=9.95623E-001 # of Data Points=361
 SS=1.14172E+007 Degrees of Freedom=357



Fitting Results

Peak Index	Peak Type	Area Intg	FWHM	Max Height	Center Grvty	Area IntgP
1	Gaussian	10657.04667	1.70012	5888.77663	284.17053	35.77487
2	Gaussian	9012.87257	1.6	5291.8928	283.3	30.25551
3	Gaussian	7176.55113	2.2	3064.50894	285.5379	24.09112
4	Gaussian	2942.72653	2.75154	1004.71227	289.1	9.8785

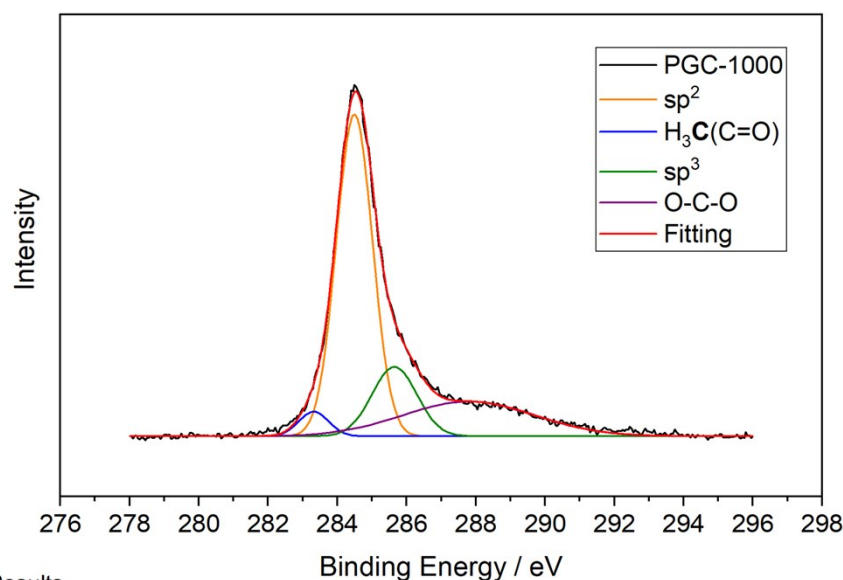
(b) BaseLine:Tougaard
 Chi²=2.64403E+004 Adj. R-Square=9.96888E-001 # of Data Points=361
 SS=9.43917E+006 Degrees of Freedom=357



Fitting Results

Peak Index	Peak Type	Area Intg	FWHM	Max Height	Center Grvty	Area IntgP
1	Gaussian	12470.72205	1.04868	11171.62642	284.3953	43.62489
2	Gaussian	1389.21008	0.78515	1662.19289	283.4152	4.85971
3	Gaussian	6751.89623	1.5046	4215.72711	285.3231	23.61938
4	Gaussian	7974.4271	4.8	1560.76171	287.7	27.89602

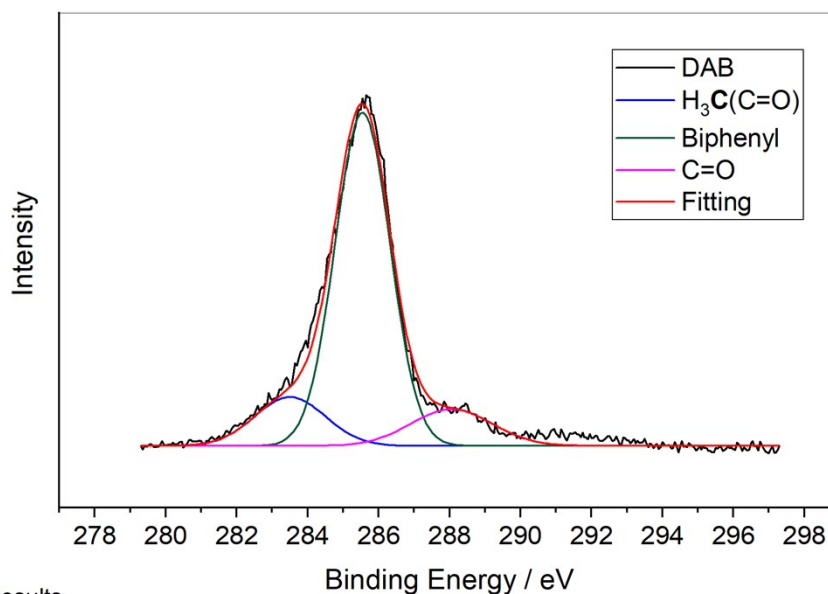
(c) BaseLine:Tougaard
 Chi²=1.60473E+004 Adj. R-Square=9.98441E-001 # of Data Points=361
 SS=5.72888E+006 Degrees of Freedom=357



Fitting Results

Peak Index	Peak Type	Area Intg	FWHM	Max Height	Center Grvty	Area IntgP
1	Gaussian	17501.5004	1.23212	13344.12388	284.4945	57.99653
2	Gaussian	1111.12896	1.02461	1018.76418	283.3207	3.68206
3	Gaussian	4673.74499	1.52725	2874.89951	285.6497	15.48787
4	Gaussian	6890.43037	4.5	1438.4856	287.7962	22.83353

(d) BaseLine:Tougaard
 Chi²=1.03005E+005 Adj. R-Square=9.91705E-001 # of Data Points=361
 SS=3.68758E+007 Degrees of Freedom=358



Fitting Results

Peak Index	Peak Type	Area Intg	FWHM	Max Height	Center Grvty	Area IntgP
1	Gaussian	4917.44618	2.34317	1971.55466	283.50466	13.93679
2	Gaussian	26101.85391	1.82187	13459.27789	285.5473	73.9766
3	Gaussian	4264.6317	2.71599	1475.09895	288.05729	12.08661

Figure S8. C 1s XPS spectra and deconvolution for (a) **PGC-Pr**, (b) **PGC-600**, (c) **PGC-1000**, and (d) **DAB**.

10. Elemental Analysis

Carbon, hydrogen, and nitrogen elemental analysis was carried out by Perkin-Elmer Model 2400 CHN Analyzer at operating temperature of 950 °C. The content of oxygen and other elements was estimated by subtracting the carbon, hydrogen, and nitrogen contents. In PGC-Pr, a relatively low carbon content was observed due to the low degree of graphitization, the presence of residual unreacted functional groups, and entrapped solvent. With higher pyrolysis temperatures, carbon content gradually increased, while hydrogen, oxygen, and other element content decreased. This observation was in consistent with the FT-IR, solid-state NMR, XPS, and conductivity results.

Table S2. Elemental analysis of **PGC-Pr**, **PGC-600**, and **PGC-1000**.

	C (%)	H (%)	N (%)	O and Other (%)
PGC-Pr	77.79	9.84	N/A	12.37
PGC-600	90.51	4.04	N/A	5.45
PGC-1000	93.91	2.84	N/A	3.25

11. Reference

- 1 D. Yuan, W. Lu, D. Zhao and H. C. Zhou, *Adv. Mater.*, 2011, **23**, 3723.
- 2 J. Jia, Z. Chen, H. Jiang, Y. Belmabkhout, G. Mouchaham, H. Aggarwal, K. Adil, E. Abou-Hamad, J. Czaban-Józwiak, M. R. Tchalala and M. Eddaoudi, *Chem*, 2019, **5**, 180.
- 3 J. Kamcev, M. K. Taylor, D. M. Shin, N. N. Jarenwattananon, K. A. Colwell and J. R. Long, *Adv. Mater.*, 2019, **31**, 1808027.
- 4 C. W. Young, R. B. DuVall and N. Wright, *Anal. Chem.*, 1951, **23**, 709.
- 5 W. Cai, R. D. Piner, F. J. Stadermann, S. Park, M. A. Shaibat, Y. Ishii, D. Yang, A. Velamakanni, S. J. An, M. Stoller, J. An, D. Chen and R. S. Ruoff, *Science*, 2008, **321**, 1815.
- 6 K. S. Yang and B.-H. Kim, *Electrochimica Acta*, 2015, **186**, 337.
- 7 S. I. Yun, H. J. Lee and B. H. Kim, *J. Electroanal. Chem.*, 2020, **858**, 113815.
- 8 N. K. Chaudhari, M. Y. Song and J. S. Yu, *Sci. Rep.*, 2014, **4**, 5221.
- 9 F. Destyorini, Y. Irmawati, A. Hardiansyah, H. Widodo, I. N. D. Yahya, N. Indayaningsih, R. Yudianti, Y.-I. Hsu and H. Uyama, *Engineering Science and Technology, an International Journal*, 2021, **24**, 514.
- 10 W. Yang, L. Hou, X. Xu, Z. Li, X. Ma, F. Yang and Y. Li, *Carbon*, 2018, **130**, 325.
- 11 S. Shi, X. Zhou, W. Chen, M. Chen, T. Nguyen, X. Wang and W. Zhang, *RSC Adv.*, 2017, **7**, 44632.
- 12 A. Gupta, S. R. Dhakate, P. Pal, A. Dey, P. K. Iyer and D. K. Singh, *Diam. Relat. Mater.*, 2017, **78**, 31.
- 13 M. Sevilla and A. B. Fuertes, *Carbon*, 2006, **44**, 468.
- 14 C. Chen, K. Sun, A. Wang, S. Q. Wang and J. C. Jiang, *Bioresources*, 2018, **13**, 3165.
- 15 B. Sivaranjini, R. Mangaiyarkarasi, V. Ganesh and S. Umadevi, *Sci. Rep.*, 2018, **8**, 8891.
- 16 L. Wang, Z. Sofer and M. Pumera, *ACS Nano*, 2020, **14**, 21.